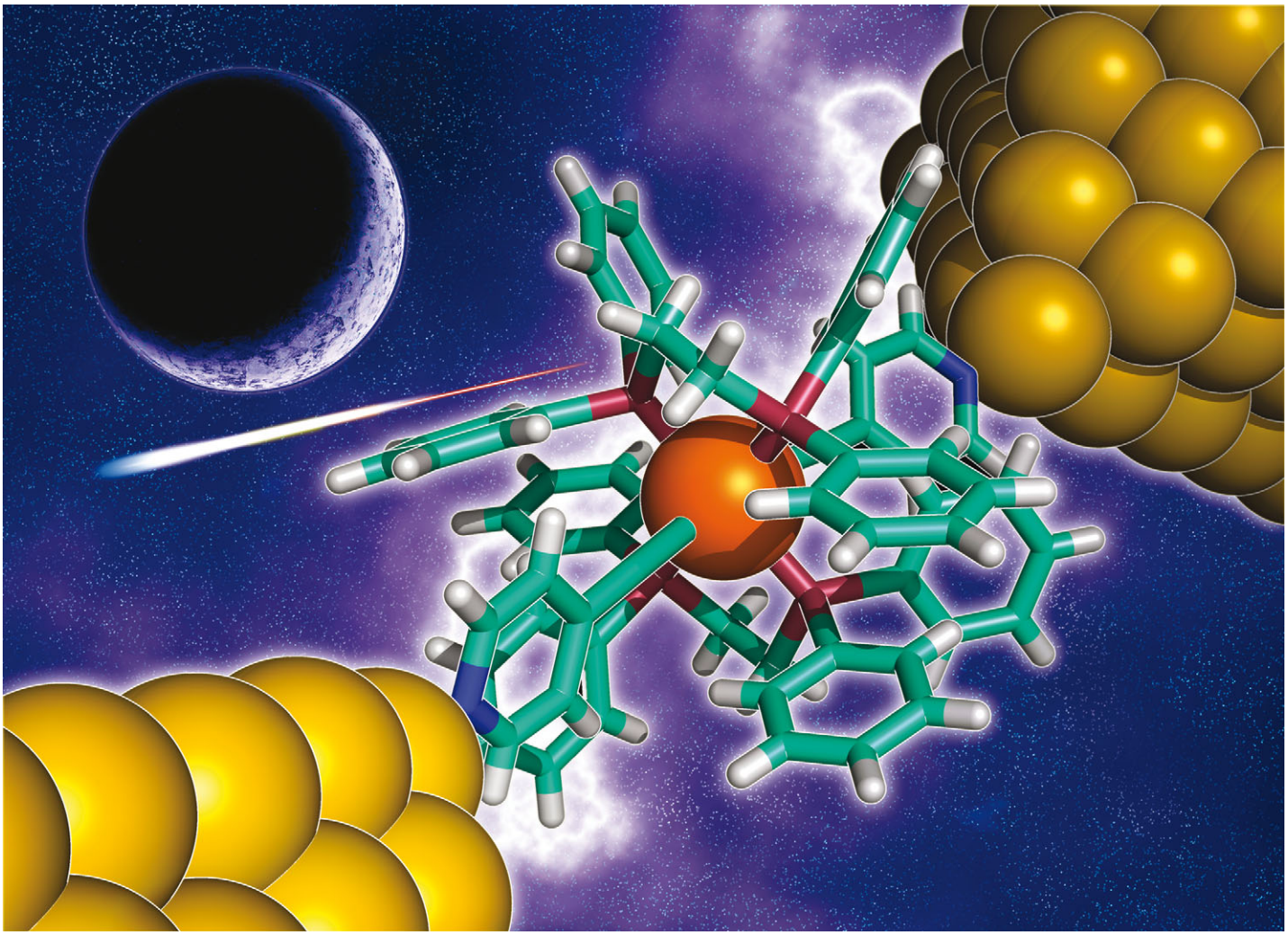

Showcasing collaborative research from the groups of Dr Yuya Tanaka and Prof. Munetaka Akita at Chemical Resources Laboratory, Prof. Manabu Kiguchi at Department of Chemistry, and Assoc. Prof. Tomofumi Tada at Materials Research Center for Element Strategy, Tokyo Institute of Technology, Japan

Organometallic molecular wires as versatile modules for energy-level alignment of the metal–molecule–metal junction

In their communication, K. Sugimoto *et al*. reveal the single molecule conductance of molecular wires in the metal–molecule–metal increases by introducing an electron-rich ruthenium fragment. Experimental and theoretical studies suggest that the high-lying HOMO is the key factor for the high-conductance.

As featured in:

See Yuya Tanaka, Tomofumi Tada, Manabu Kiguchi, Munetaka Akita *et al*., *Chem. Commun*., 2016, **52**, 5796.

ROYAL SOCIETY OF CHEMISTRY

www.rsc.org/chemcomm

Registered charity number: 207890

ChemComm

COMMUNICATION

View Article Online
View Journal | View Issue

Cite this: *Chem. Commun.*, 2016, 52, 5796

Received 25th February 2016,
Accepted 10th March 2016

DOI: 10.1039/c6cc01705c

www.rsc.org/chemcomm

Organometallic molecular wires as versatile modules for energy-level alignment of the metal–molecule–metal junction†

Kaho Sugimoto,[a] Yuya Tanaka,*[a] Shintaro Fujii,[b] Tomofumi Tada,*[c] Manabu Kiguchi*[b] and Munetaka Akita*[a]

The organometallic Ru molecular wires 1–3 $Ru(PR_3)_4(C{\equiv}CC_5H_5N)_2$ [$(PR_3)_4$ = $(dppe)_2$ (1), $[P(OMe_3)]_4$ (2), and $(dmpe)_2$ (3)] show significantly higher conductance compared to their organic counterpart, 1,4-dipyridyl butadiyne (4). CV and UV-Vis measurements and DFT calculations suggest that the high-lying HOMOs of the Ru wires are the key factor for the high conductance.

Understanding the principles of charge transport through metal (electrode)–molecule–metal (electrode) junctions is of fundamental importance in the field of molecular electronics.[1] Recent efforts devoted toward single molecule conductance measurements of organic molecular wires, which are composed of an organic linker with two anchoring units to be attached to electrodes (Fig. 1a), have shown that the conductance significantly varies depending on the molecular structures, and systems with π-conjugated linkers are generally superior to those without a π-system.[2] An important issue to be resolved for the molecular wires is the length-dependent deterioration of the conductance (*e.g.* relatively large attenuation factors β) when the coherent tunneling process is dominant.[3] One of the reasons for this is the energy mismatch between the frontier molecular orbitals (frontier MOs) and the Fermi level (E_F) of the electrodes.[4]

Various efforts to align the frontier MO energies and E_F have been made, including narrowing of the HOMO–LUMO gaps *via* expansion of the π-system,[3,5] introducing electron-donating/withdrawing substituents,[6] and metal coordination.[7] In general, when the charge transport mechanism is dominated by LUMO conduction (n-type conductor), the molecular conductance increases by stabilizing the LUMO by, for example, by the introduction of electron-withdrawing substituents or coordination of Lewis acidic metals, and *vice versa* for HOMO conducting systems (p-type conductor). The dominant conducting orbital is generally dependent on the anchoring units.[8] The challenge is to find suitable methods to improve molecular conductance regardless of the anchoring groups, though such a universal module has not been reported to date.

The electron-rich d^8 metal acetylide complexes, which are widely studied for their long-range intramolecular, intermetallic electron transfer properties,[9] are suitable specimens to modify

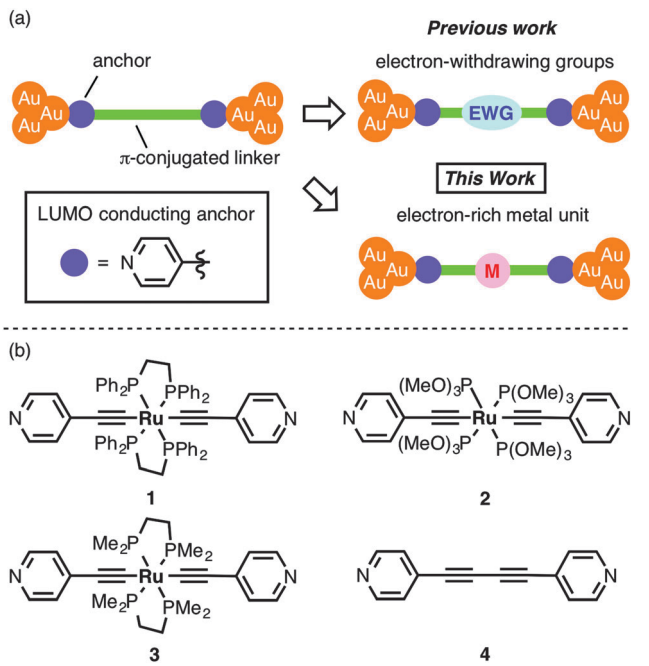

Fig. 1 (a) Schematic representations of the molecular junctions of organic wires and strategies to improve molecular conductance of the molecular wires with pyridine anchoring groups. (b) The molecular structures of **1–4**.

[a] *Chemical Resources Laboratory, Tokyo Institute of Technology, R1-27, 4259 Nagatsuta Midori-ku, Yokohama 226-8503, Japan. E-mail: ytanaka@res.titech.ac.jp, makita@res.titech.ac.jp*
[b] *Department of Chemistry, Graduate School of Science and Engineering, Tokyo Institute of Technology, 2-12-1 W4-10, Ookayama, Meguro-ku, Tokyo 152-8551, Japan. E-mail: kiguti@chem.titech.ac.jp*
[c] *Materials Research Center for Element Strategy, Tokyo Institute of Technology, 4259 Nagatsuta-cho, Midori-ku, Yokohama, Kanagawa 226-8503, Japan. E-mail: tada.t.ae@m.titech.ac.jp*

† Electronic supplementary information (ESI) available: Experimental and computational details are involved. CCDC 1442139. For ESI and crystallographic data in CIF or other electronic format see DOI: 10.1039/c6cc01705c

the conductance properties of π-conjugated organic molecular wires, because (1) strong interaction of the π-conjugated systems through the central metal atom results from the metal–carbon dπ–pπ interactions, and (2) the metal unit directly affects frontier MOs with a large metal character. Therefore it is reasonable that single molecule conductance of the electron-rich d^8 metal acetylide systems with HOMO conducting anchors has been reported to be enhanced as a result of the orbital alignment of the HOMO with E_F.[10] Such a successful strategy has been extended even to oligomeric metal-acetylide systems as reported by Rigaut, Frisbie and Chen,[11] and Berke, Riel and Lörtscher[12] as well as to other related metal complexes.[13] Herein, we report single molecule conductance of the Ru acetylide system with pyridine anchoring groups, which prefer electron transport through the LUMO,[14] and show that the electron-rich Ru fragments are versatile modules to align energy-levels in the metal–molecule–metal junctions.

Three organometallic molecular wires with the ethynylpyridine anchors connected to the $Ru(PR_3)_4$ units **1–3** having different electronic and steric features were prepared (Fig. 1b), and their octahedral trans-coordination geometries have been characterized spectroscopically and, for **1**, crystallographically (Fig. 2). The trend observed for the $\nu(C\equiv C)$ vibration [2052 (**3**), 2056 (**1**), and 2073 cm^{-1} (**2**)] indicates that, as the electron-donating property of the PR_3 ligands becomes stronger, the C≡C vibrational frequency shifts to the lower energies as a result of an increase of π-back donation from the Ru atom to the C≡C moiety. Averaged Ru–C (2.06 Å) and C≡C distances (1.21 Å) observed for **1** are within the normal ranges observed for related derivatives.[15] The N–N separation is 1.49 nm.‡

Single molecule conductance measurements were performed using the STM-break junction (STM-BJ) method. This method was first developed by Tao[16] and is currently regarded as a reliable method to measure single molecule conductance.[17] The details of the experimental conditions are described in ref. 18. No plateau is observed for the solvent, tetraglyme (Fig. 3a), and the histogram does not show any reproducible peaks (Fig. 3e). In contrast, a tetraglyme solution containing **1** shows plateaus at the individual traces (Fig. 3b). A histogram constructed from

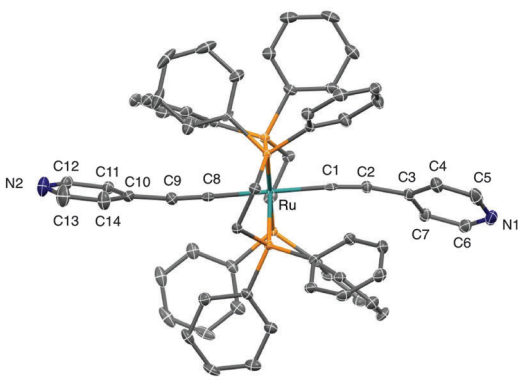

Fig. 2 X-ray structure of **1**. Hydrogen atoms are omitted for clarity. Selected bond lengths (in Å): Ru–C1 2.061(3), Ru–C8 2.068(3) C1–C2 1.207(4), C8–C9 1.207(4), Ru–N1 7.440(3), Ru–N2. 7.521(3), N1–N2 14.914(4).

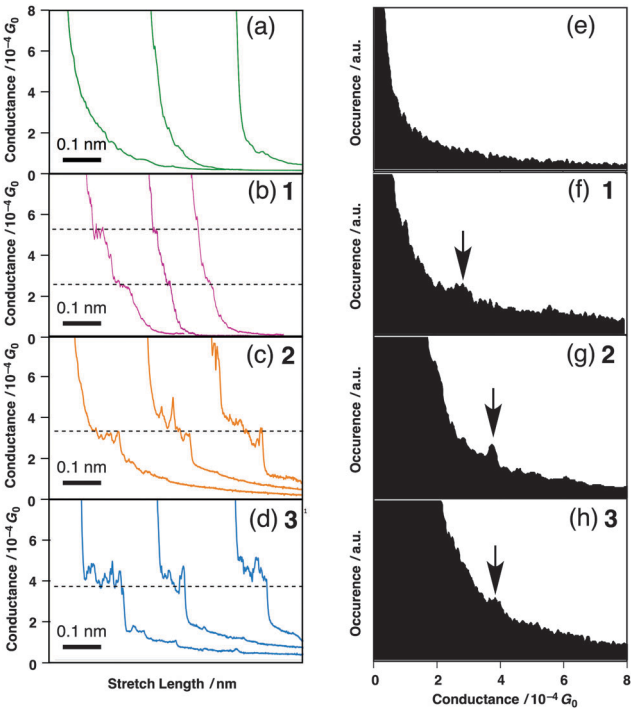

Fig. 3 Typical conductance traces and 1D histograms of the solvent (a and e), **1** (b and f), **2** (c and g), and **3** (d and h). The dotted lines correspond to each molecular conductance and the arrows indicate the position of the molecular conductance. Bias voltage was applied at 100 mV.

100 individual traces gives a reproducible peak at 2.5 (±0.4) × 10^{-4} G_0 (Fig. 3f), where 1 G_0 ($2e^2/h$ = 77.5 μS) is the quantum conductance. Therefore, the result confirms that the observed peak is derived from the molecule. The lengths of the steps observed for the individual traces, which indicate the contact period of the molecular junction, are much shorter than the molecular length of **1** probably due to the sterically bulky dppe ligands.[18] Similarly, complexes **2** and **3** show peaks at 3.8 (±0.8) × 10^{-4} and 3.9 (±0.3) × 10^{-4} G_0, respectively (Fig. 3c, d, g and h). The obtained values are significantly larger than that for the organic reference compound **4** [1.0 (±0.2) × 10^{-4} G_0],[3,18] despite the N–N separation (*ca.* 1.5 nm) being longer than that for the organic wire **4** (*ca.* 1.2 nm). Because the terminal anchoring groups are identical for **1–4**, the difference of the conductance can be ascribed to the organometallic units embedded, indicating that the organometallic units promote carrier transfer through the metal–molecule–metal junctions in an efficient manner.

In order to get insight into the origin of the high conductance of the Ru wires **1–3**, frontier MOs of the molecules were analyzed (Fig. 4), and conductive frontier MOs were examined. Orbital level analysis was also done using a combination of cyclic voltammetry and UV-Vis spectroscopy, and the results are listed in Table 1. The experimental values for the HOMO levels of **1–3** were estimated to be in the range of −5.0 to −5.5 eV, which are higher than that of **4** by ∼2 eV. Similarly, the LUMO levels of the Ru complexes **1–3** are higher than that of **4** by 0.7–1.6 eV, indicating that the electron donating Ru units destabilizes both HOMOs and LUMOs as expected. The HOMO and LUMO of **4**

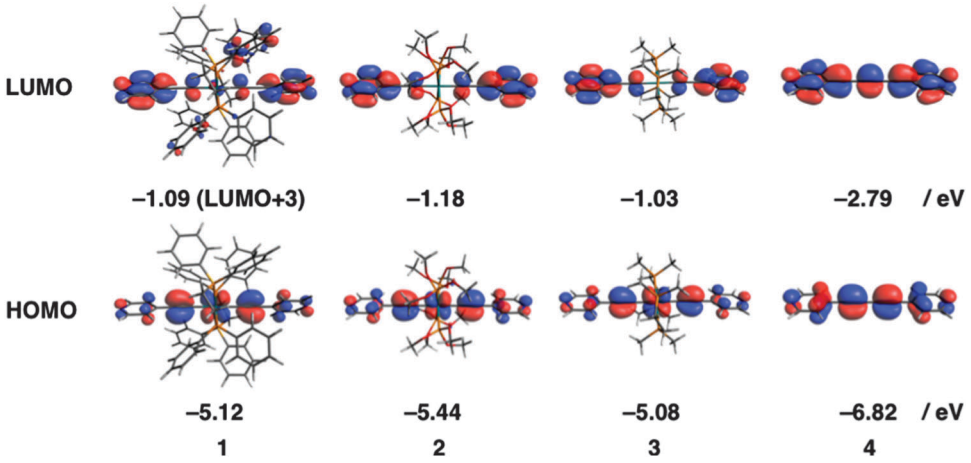

Fig. 4 Kohn–Sham orbitals and orbital energies of **1–4**. The orbitals were calculated at the B3LYP/LanL2DZ(Ru), 6-311+G(d,p) (C, H, N, P)//B3LYP/LanL2DZ(Ru),6-31G(d) (C, H, N, P) levels of theory. For **1**, LUMO+3 is shown.[19]

Table 1 Experimental and calculated single molecule conductance and frontier orbital energies of **1–4**

Compound	**1**	**2**	**3**	**4**
Conductance (Exp./Calcd)/10^{-4} G_0	2.5 (±0.4)/17.1	3.8 (±0.8)/10.4	3.9 (±0.3)/9.7	1.0 (±0.2)/8.3
E_{HOMO}[a]/eV	−5.22	−5.52	−5.05	−7.17
E_{LUMO}[b]/eV	−1.91	−2.75	−1.86	−3.41
$E_{HOMO-LUMO}$[c]/eV	3.31	2.77	3.19	3.76

[a] Estimated by CV. [b] LUMO energies (E_{LUMO}) were obtained by the following equation. $E_{LUMO} = E_{HOMO} + E_{HOMO-LUMO}$. [c] Estimated by UV-Vis absorption spectra.

obtained using hybrid Density Functional Theory (DFT) calculations mainly consist of π-orbitals, which are delocalized over the whole molecules. For the Ru wires **1–3**, similar delocalized orbitals are found for HOMOs with antibonding dπ–pπ interactions between the Ru and acetylene α-carbon atoms. In sharp contrast, as shown in Fig. 4, orbital distribution of LUMOs of **1–3** are different from that for **4**. As mentioned above, the LUMO of **4** is delocalized over the whole π-conjugated system, while, for LUMO+3 of **1** and LUMOs of **2** and **3**, contribution of the Ru atoms is negligible.[19] Considering that (1) the HOMO and LUMO of the Ru wires are destabilized compared to **4** and (2) delocalization of the LUMOs of **1–3** is disconnected by the Ru atom, the HOMOs, instead of the LUMO, should play important roles in the high conductance of **1–3**.

In order to clarify the conducting orbital state for the metal–molecule–metal junctions, we carried out hybrid DFT calculations coupled with non-equilibrium Green's function method for molecular wires attached to two triangular pyramidal Au clusters (Au_{35}) as shown in Fig. 5.[20] The modeled molecular junctions of **1–4** are denoted as Au-**1**-Au *etc.* The calculated zero bias conductance of the Ru wires **1–3** (17.1, 10.4, 9.7 × 10^{-4} G_0) is higher than that of **4** (8.3 × 10^{-4} G_0), which is roughly in accordance with the experimental results (**1**, **2**, **3** > **4**). Fig. 5a shows the transmission spectra for the Au-(**1–4**)-Au junctions. Transmission peaks around 1–2 eV located above E_F can be attributed to the LUMOs as shown in Fig. 5b. The HOMO-derived peaks for **4** are found around 2–3 eV located below E_F, whereas those for **1–3** are found to be around −1 to −2 eV; Fig. 5a shows that four MOs of **1** are formed in the energy range, and the most conductive MO is depicted in Fig. 5b. That is, the HOMOs of the Ru-wire molecular junctions are closer in energy to the Fermi level (E_F) of the electrodes, as expected from the calculations of the isolated molecules (see above). These features, therefore, strongly suggest that the conductance of Ru wires **1–3** increases due to larger contributions of the high-lying HOMOs as the conduction orbitals.[6] The origin of the difference in the conductance for **1–3** is still unclear; not only an accurate description of the electronic structure for Ru-complexes but also other factors involving structural arrangements might be needed for the detailed analysis of the conduction.[21] Indeed, the pyridine rings of complex **1** are twisted due to the steric hindrance of the dppe fragments as found for the X-ray and DFT optimized structures, suggesting that the conformational flexibility of the ethynylpyridine parts is limited, while essentially no steric hindrance has been found for **2** and **3**.[18]

In summary, we have shown that the single molecule conductance performance of Ru wires **1–3** with pyridine anchoring groups is superior to the corresponding organic counterpart **4** despite the molecular dimensions of the Ru wires being longer than that of **4**. The origin of the high conductance is the high-lying HOMO, which is distributed over the whole molecule. The presented results are in contrast to the common molecular design used to improve the performance of molecular wires using a LUMO conducting system, *i.e.* stabilizing the LUMO energy by introducing electron-deficient units or substituents. Therefore, the incorporation of an electron-rich metal unit can be a versatile method to enhance conductivity of molecular wires with both HOMO and LUMO conducting anchoring groups.

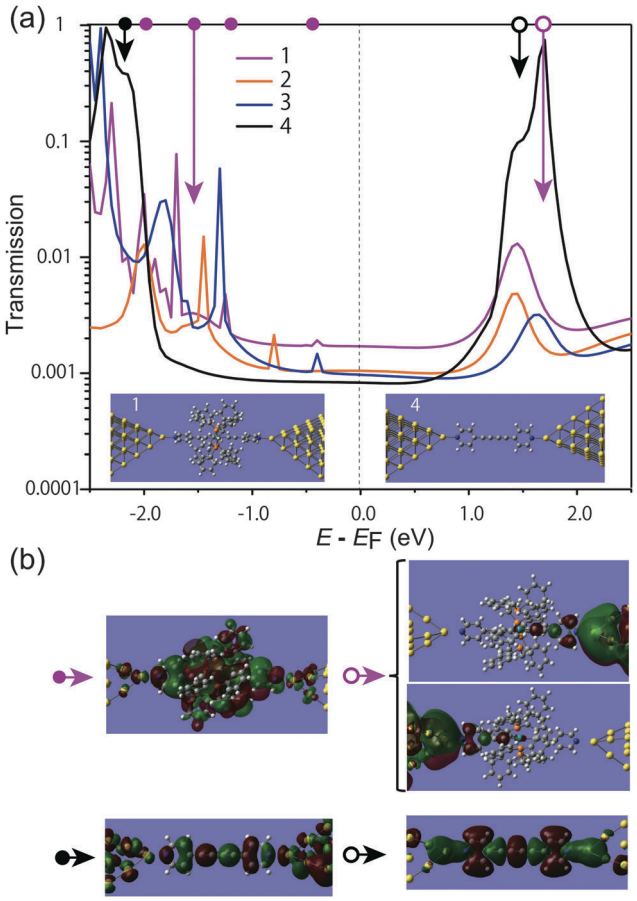

Fig. 5 Calculated transmission spectra and molecular junction models. (a) Transmission spectra of Au-**1**-Au, Au-**2**-Au, Au-**3**-Au, and Au-**4**-Au, and junction configurations of Au-**1**-Au and Au-**4**-Au (inset). The positions of conductive molecular orbitals are indicated with a filled/unfilled circle and an arrow. (b) Conductive molecular orbitals of Au-**1**-Au and Au-**4**-Au. Three pink filled circles in (a) are also π-orbitals, but the couplings with electrodes are weaker than that of conducting MO.

This work was supported by JSPS KAKENHI Grant Number 26810031. The computations were performed partly by using Research Center for Computational Science, Okazaki, Japan, and using the TSUBAME2.5 supercomputer in Tokyo Institute of Technology.

Notes and references

‡ Crystal data of **1**·CH_2Cl_2 (CCDC number 1442139). $C_{67}H_{58}Cl_2N_2P_4Ru$, M = 1187.01, triclinic, a = 10.5042(9), b = 12.4115(11), c = 22.3482(19) Å, U = 2754.9(4) Å^3, T = 110(2) K, space group $P\bar{1}$ (no. 2), Z = 2, 13071 reflections measured, 9739 unique (R_{int} = 0.014), which were used for all calculations. The final wR($F2$) was 0.120 (all data).

1 C. Joachim, J. K. Gimzewski and M. A. Aviram, *Nature*, 2000, **408**, 541; A. Nitzan and M. A. Ratner, *Science*, 2003, **300**, 1384.
2 Y. Li, J. Zhao, X. Yin and G. Yin, *J. Phys. Chem. A*, 2006, **110**, 11130.
3 P. Moreno-García, M. Gulcur, D. Z. Manrique, T. Pope, W. Hong, V. Kaliginedi, C. Huang, A. S. Batsanov, M. R. Bryce, C. Lambert and T. Wandlowski, *J. Am. Chem. Soc.*, 2013, **135**, 12228.
4 H. Liu, N. Wang, J. Zhao, Y. Guo, X. Yin, F. Y. C. Boey and H. Zhang, *ChemPhysChem*, 2008, **9**, 1416.
5 G. Sedghi, V. M. García-Suárez, L. J. Esdaile, H. L. Anderson, C. J. Lambert, S. Martin, D. Bethell, S. J. Higgins, M. Elliott, N. Bennett, J. E. Macdonald and R. J. Nichols, *Nat. Nanotechnol.*, 2011, **6**, 517.
6 L. Venkataraman, Y. S. Park, A. C. Whalley, C. Nuckolls, M. S. Hybertsen and M. L. Steigerwald, *Nano Lett.*, 2007, **7**, 502.
7 J. Ponce, C. R. Arroyo, S. Tatay, R. Frisenda, P. Gavina, D. Aravena, E. Ruiz, H. S. J. van der Zant and E. Coronado, *J. Am. Chem. Soc.*, 2014, **136**, 8314.
8 J. R. Widawsky, P. Darancet, J. B. Neaton and L. Venkataraman, *Nano Lett.*, 2012, **12**, 354.
9 J.-F. Halet and C. Lapinte, *Coord. Chem. Rev.*, 2013, **257**, 1584; M. I. Bruce and P. J. Low, *Adv. Organomet. Chem.*, 2004, **50**, 179; P. J. Low, *Coord. Chem. Rev.*, 2013, **257**, 1507; M. Akita and T. Koike, *Dalton Trans.*, 2008, 3523; S. Szafert and J. A. Gladysz, *Chem. Rev.*, 2006, **106**, PR1; K. Costuas and S. Rigaut, *Dalton Trans.*, 2011, **40**, 5643.
10 K. Liu, X. Wang and F. Wang, *ACS Nano*, 2008, **2**, 2315; S. Marqués-González, D. S. Yufit, J. A. K. Howard, S. Martín, H. M. Osorio, V. M. García-Suárez, R. J. Nichols, S. J. Higgins, P. Ceacd and P. J. Low, *Dalton Trans.*, 2013, **42**, 338.
11 B. S. Kim, J. M. Beebe, C. Olivier, S. Rigaut, D. Touchard, J. G. Kushmerick, X.-Y. Zhu and C. D. Frisbie, *J. Phys. Chem. C*, 2007, **111**, 7521; F. Meng, Y.-M. Hervault, L. Norel, K. Costuas, C. V. Dyck, V. Geskin, J. Cornil, H. H. Hng, S. Rigaut and X. Chen, *Chem. Sci.*, 2012, **3**, 3113; F. Meng, Y.-M. Hervault, Q. Shao, B. Hu, L. Norel, S. Rigaut and X. Chen, *Nat. Commun.*, 2014, **5**, 3023.
12 F. Lissel, F. Schwarz, O. Blacque, H. Riel, E. Lörtscher, K. Venkatesan and H. Berke, *J. Am. Chem. Soc.*, 2014, **136**, 14560; F. Schwarz, G. Kastlunger, F. Lissel, H. Riel, K. Venkatesan, H. Berke, R. Stadler and E. Lörtscher, *Nano Lett.*, 2014, **14**, 5932; F. Schwarz, G. Kastlunger, F. Lissel, C. Egler-Lucas, S. N. Semenov, K. Venkatesan, H. Berke, R. Stadler and E. Lörtscher, *Nat. Nanotechnol.*, 2016, **11**, 170.
13 S. Ballmann, W. Hieringer, D. Secker, Q. Zheng, J. A. Gladysz, A. Görling and H. B. Weber, *ChemPhysChem*, 2010, **11**, 2256.
14 E. Leary, A. La Rosa, M. T. González, G. Rubio-Bollinger, N. Agraïtab and N. Martín, *Chem. Soc. Rev.*, 2015, **44**, 920.
15 Z. Atherton, C. W. Faulkner, S. L. Ingham, A. K. Kakkar, M. S. Khan, J. Lewis, N. J. Long and P. R. Raithby, *J. Organomet. Chem.*, 1993, **462**, 265.
16 B. Xu and N. J. Tao, *Science*, 2003, **301**, 1221.
17 M. Kiguchi and S. Kaneko, *Phys. Chem. Chem. Phys.*, 2013, **15**, 2253; V. Kaliginedi, A. V. Rudnev, P. Moreno-Garcia, M. Baghernejad, C. Huang, W. Hong and T. Wandlowski, *Phys. Chem. Chem. Phys.*, 2014, **16**, 23529; S. V. Aradhya and L. Venkataraman, *Nat. Nanotechnol.*, 2013, **8**, 399.
18 See the ESI†.
19 LUMO+3 is shown, because LUMO − LUMO+2 are dppe-based orbitals. For details, see the ESI†.
20 T. Tada, M. Kondo and K. Yoshizawa, *J. Chem. Phys.*, 2004, **121**, 8050.
21 S. Marqués-González, M. Parthey, D. S. Yufit, J. A. K. Howard, M. Kaupp and P. J. Low, *Organometallics*, 2014, **33**, 4947.